ACS APPLIED MATERIALS & INTERFACES

Letter

www.acsami.org

Fabrication of Thin Films of α-Fe_2O_3 via Atomic Layer Deposition Using Iron Bisamidinate and Water under Mild Growth Conditions

Jason R. Avila,[†,§] Dong Wook Kim,[†,§] Martino Rimoldi,[†] Omar K. Farha,[*,†,§,‡] and Joseph T. Hupp[*,†,§,⊥]

[†]Department of Chemistry, Northwestern University, 2145 Sheridan Road, Evanston, Illinois 60208, United States

[‡]Department of Chemistry, Faculty of Science, King Abdulaziz University, Jeddah, Saudi Arabia

[§]Argonne-Northwestern Solar Energy Research (ANSER) Center, Northwestern University, 2145 Sheridan Road, Evanston, Illinois 60208, United States

[⊥]Argonne National Laboratory, 9700 South Cass Avenue, Argonne, Illinois 60439, United States

Supporting Information

ABSTRACT: Atomic layer deposition (ALD) has been shown to be an excellent method for depositing thin films of iron oxide. With limited iron precursors available, the methods widely used require harsh conditions such as high temperatures and/or the use of oxidants such as ozone or peroxide. This letter aims to show that bis(N,N′-di-t-butylacetamidinato) iron(II) (iron bisamidinate or FeAMD) is an ideal ALD precursor because of its reactivity with water and relative volatility. Using in situ QCM analysis, we show outstanding conformal self-limiting growth of FeO_x using FeAMD and water at temperatures lower than 200 °C. By annealing thin films of FeO_x at 500 °C, we observe the formation of α-Fe_2O_3, confirming that we can use FeAMD to fabricate thin films of catalytically promising iron oxide materials using moderate growth conditions.

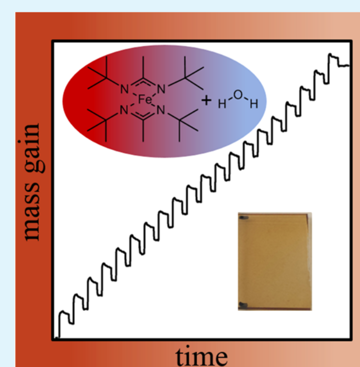

KEYWORDS: *atomic layer deposition, quartz crystal microbalance, in situ, iron oxide, hematite, iron bisamidinate*

From their natural abundance to low toxicity, iron oxide-based materials have shown great promise for a variety of applications including homogeneous catalysis, heterogeneous photoelectrochemical catalysis, energy storage, and the development of magnetic materials.[1−3] Nanostructuring has the potential to increase the performance of materials in all of these applications by increasing (or stabilizing) the number of active sites for catalysis for example, or by decreasing the charge collection length for applications such as photoelectrochemical oxidation of water.[4−8] One way to maximize charge collection of nanostructured materials is through using a thin film of active material on high surface area conductive scaffold.[7,9,10] Atomic layer deposition (ALD) is a chemical vapor deposition technique used to grow thin, conformal films of metals, oxides, nitrides, and sulfides.[11,12] These uniform films are grown by exposing reactive precursors to a substrate containing spatially separated terminal functional groups (such as hydroxyl or thiol groups) that promote precursor mixing solely at the surface of the material. This method allows for films to be grown in a self-limiting manner that gives rise to atomic level control over both thickness and composition.[11,12] This unique gas phase mechanism allows for conformal deposition of materials on highly porous substrates with high aspect ratio. Conventionally, growth of metal oxides by ALD requires the use of two precursors: a reactive metal compound and an oxygen source. By alternating exposure of the substrate to the metal source and oxygen source, a film of metal-oxide material can be easily grown layer by layer. Unfortunately, there are limited number of iron ALD precursors available that can be used at low temperature, and many require nonideal conditions such as use of an oxidant. The most ubiquitous recipe currently used for depositing iron oxide by ALD involves the use of ferrocene.[7,9,13−19] Although fairly low in cost, the high stability of ferrocene as a precursor requires the use of ozone or high temperature (350−500 °C) to remove the cyclopentadienyl ligands for further Fe deposition.[12] The drawbacks of the ferrocene/ozone mixtures are plentiful including reactor profiling, high temperature for growth, and regular costly maintenance of the ALD tool and pump because of condensation of ferrocene; see the Supporting Information. An intriguing alternative precursor is bis(2,4-methylpentadienyl) iron, as shown by Riha and co-workers.[20] This precursor has the benefit of reacting with O_2 and H_2O_2. This Fe complex shows great promise due to its reactivity at low temperature but does suffer from degradation at higher temperatures. As a consequence, vapor boost assistance is required in order to volatilize the precursor without destroying it, which limits its use on most commercial systems. To open up the possibility of growing iron oxide in or around organic materials,[11,21,22] a

Received: May 10, 2015
Accepted: July 20, 2015
Published: July 20, 2015

 © 2015 American Chemical Society

DOI: 10.1021/acsami.5b04043
ACS Appl. Mater. Interfaces 2015, 7, 16138−16142

water reactive iron compound would be the best candidate for ALD.

Of the few precursors used to grow iron oxide by ALD, there are even fewer that have been shown to react with water. $FeCl_3$ is the most likely candidate given that it readily reacts with water. Indeed, $FeCl_3$ has been shown to possess relatively high growth rates with water, but it requires high temperatures to avoid precursor condensation and the incorporation of excess Cl in the films.[23] Additionally, the presence of HCl vapor as a byproduct of the $FeCl_3/H_2O$ reaction can have detrimental effects on the ALD instrument safety seals. Alternatively, $Fe_2(OtBu)_6$ has been proposed as a water reactive ALD precursor for the formation of iron oxide but in our hands the precursor requires a synthetic impurity and multiple pulses for nucleation and growth to be observed.[1] This behavior points to a $FeCl_3$ impurity in the $Fe_2(OtBu)_6$, which needs to be present for ALD growth of iron oxide. As a result, this precursor suffers from the same limitations as those mentioned previously. Among the best candidate precursors for water reactive growth of interesting metal oxides by ALD are the bisamidinate compounds developed by Gordon and co-workers.[24] These bisamidinate compounds have been shown to make metals and metal oxides by reacting with H_2 and H_2O, respectively, and they have opened up the ability to grow a wide variety of transition metal oxide films at low temperatures.[10,25] Despite the potential of iron bisamidinate (FeAMD), see Figure 1, for the growth of iron oxide by ALD, no studies involving the growth or characterization of iron oxide films using this precursor at temperatures below 200 °C have been reported. The goal of this report is to illustrate the benefits of FeAMD toward the formation of thin-film α-Fe_2O_3 (hematite), grown at low temperatures using water as the oxygen source.

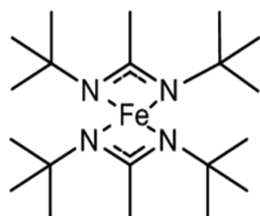

Figure 1. Bis(N,N′-di-t-butylacetamidinato) iron(II) precursor used for ALD of FeO, referred to as iron bisamidinate or FeAMD.

ALD of iron oxide (FeO) using FeAMD was implemented on a Savannah 200 (Ultratech) commercial ALD reactor modified with a wall mounted quartz crystal microbalance (QCM) to measure film growth in situ.[26] Figure 2 summarizes the growth rate of the FeAMD precursor on our system measured by QCM. As shown in Figure 2, we observe an average growth rate of 0.55 ± 0.05 Å/cycle. This growth rate is more than 0.2 Å/cycle higher than that reported by Lim and co-workers[24] likely due to the lower reactor temperatures used here, which has been observed for other ALD processes.[21,27,28] Figure 2a also shows the importance of using a long purge time (30 s) in order to sufficiently clear the reactor of precursor and to avoid undesirable CVD reactions, with 15 s showing a higher average growth rate and more variations between runs. In contrast, variations in pulse time and reactor temperature have negligible effect on the growth rate with the exception of a slight profile observed for 0.1 s pulse and 130 °C reactor temperature as shown in Figure 2b, c. The wall-mounted QCM used in this study was equipped with 2 ports, one near the reactor inlet and outlet to observe if any growth profile was observed during the ALD process. As summarized in Figure S1 in the Supporting Information, there is a minimal growth difference between the inlet and outlet of the ALD reaction, with a maximum growth difference of ~0.1 Å/cycle (conveyed in the error values used in Figure 2). The source of this growth profile is attributed to temperature variations in reactor which would cause small differences in growth rate throughout the reactor, which is commonly observed in our hands. The greatest growth profile was observed for the 20 s purge time which, as previously mentioned, is due to insufficient time to remove physisorbed FeAMD precursor, causing significant CVD near the inlet of the reactor. See the Supporting Information, Figure S1, for further discussion on the minimal growth profile observed in this study.

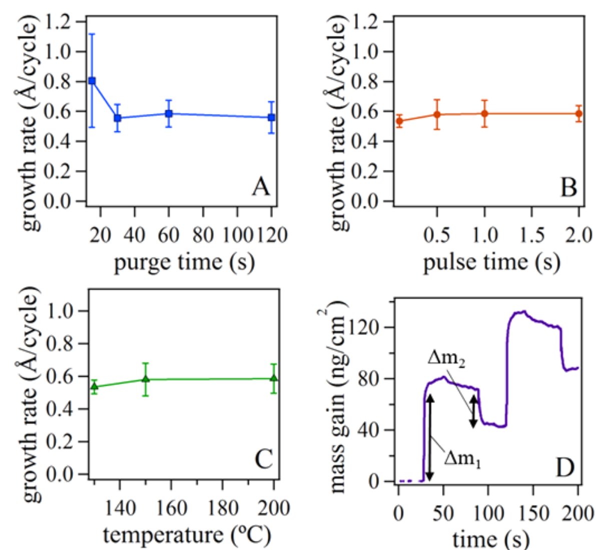

Figure 2. (a) Growth rate as a function of precursor purge time with a 1 s pulse time and reactor temperature of 150 °C. (b) Growth rate as a function of precursor pulse time with a 60 s precursor purge time and 150 °C reactor temperature. (c) Growth rate as a function of reactor temperature with a precursor pulse time of 1 s and purge time of 60 s. (d) Zoom in of QCM trace showing mass change upon FeAMD precursor pulse (Δm_1) and water pulse (Δm_2). In all cases, FeAMD was kept at 120 °C and water was pulsed for 15 ms and purged for 30 s. Growth rates were averaged from traces measured near the inlet and outlet of the reactor.

The trace in Figure 2d indicates a deposition of approximately 71 ng/cm^2 with the FeAMD (Δm_1) pulse and loss of ~42 ng/cm^2 during water pulsing (Δm_2). The observed 58% drop in mass upon exposure to water is in good agreement with that expected from the loss of the amidinate ligand in addition together with the acquisition of 2 or 3 aqua and/or hydroxy groups per iron center (53−63% mass loss). The full QCM trace corresponding to Figure 2d can be found in the Supporting Information, Figure S2, and shows a linear growth rate for all cycles deposited. The self-limiting nature of the precursor was confirmed by observation of a saturation in mass gain upon the second FeAMD pulse without using water to complete the cycle, (Figure S3 in the Supporting Information). From the information summarized in Figure 2, we can confirm that the precursor grows consistently in a self-limiting fashion with a growth rate of 0.55 ± 0.05 Å/cycle. Vapor pressure regeneration of the precursor is shown to be the sole reason for any reactor profiling observed (see the Supporting Information,

DOI: 10.1021/acsami.5b04043
ACS Appl. Mater. Interfaces 2015, 7, 16138−16142

Figure S4, for details), and can be solved with longer purge times or higher precursor temperatures. We have also observed a growth rate of 0.12 ± 0.02 Å/cycle with O_2 instead of H_2O indicating the faster growth mechanism is one that maximizes the formation of hydroxo groups over precursor oxidation (see the Supporting Information, Figure S5, for QCM trace).[29]

Because of the promising applications[2] of α-Fe_2O_3 (hematite), we annealed thin films (5 to 19 nm) of FeO_x, grown using FeAMD ALD, and found that we can obtain films with quality and crystalline phase equivalent to that of iron oxide films grown using other ALD methods. Figure 3 shows

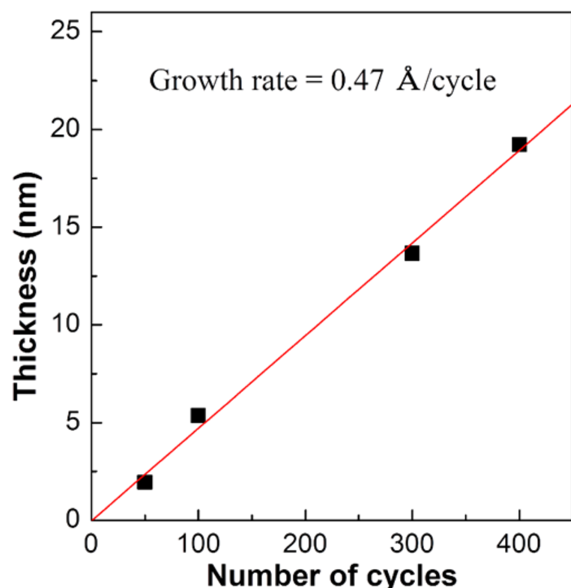

Figure 3. Correlation between α-Fe_2O_3 film thickness and the number of ALD cycles as monitored by ellipsometry. The films are grown on Si substrates at 150 °C, and then annealed at 500 °C in air.

the ellipsometry-determined thickness of α-Fe_2O_3 films formed by annealing FeO_x ALD films in air at 500 °C demonstrating that there is an excellent linear correlation between the total FeAMD-H_2O ALD cycles and the thickness of α-Fe_2O_3 measured. The growth rate of 0.47 ± 0.02 Å/cycle determined from ellipsometry is close to that estimated by QCM, with the difference likely arising from the assumed density of FeO used to calculated the thickness in the QCM measurement (see the Supporting Information).

In order to confirm the structure of the fabricated iron oxide films, grazing incidence X-ray diffraction (GIXRD) and X-ray photoelectron spectroscopy (XPS) measurements were made. As revealed in Figure 4, the as-synthesized films are amorphous, whereas the annealed films show the presence of crystalline α-Fe_2O_3, regardless of thickness. XPS spectra (Figure S6 in the Supporting Information)m however, show that the binding energies of Fe $2p_{3/2}$ main line and its satellite peak for the as-synthesized film are identical to those of the annealed film. In addition, the satellite peak of Fe $2p_{3/2}$ is observed at 719 eV, indicating the presence of only Fe(III) in both the as-synthesized and annealed films. This indicates surface oxidation by atmospheric O_2 readily occurs on amorphous FeO_x films grown by ALD using FeAMD-H_2O and crystallize into α-Fe_2O_3 via calcination at 500 °C despite the thinness the films. The synthesis of crystalline α-Fe_2O_3 films as thin as 5 nm could be particularly useful in electrochemical applications, because the

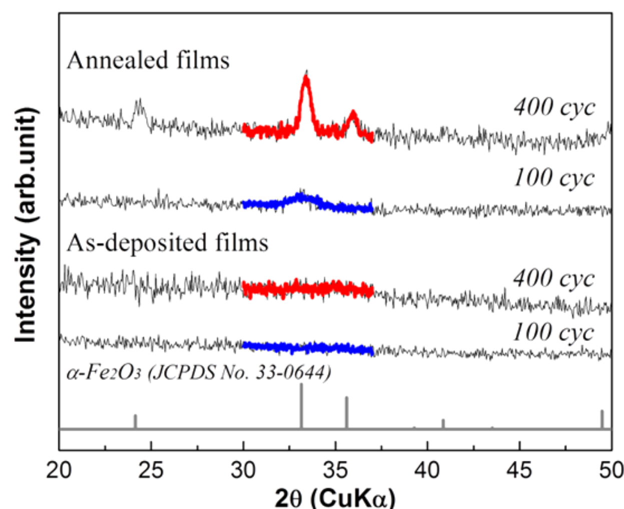

Figure 4. Grazing incidence XRD patterns of a 5 (blue) and 19 (red) nm thick films deposited on Si and annealed at 500 °C. Thicker lines show slow scan diffraction patterns in the range of 30−37. All of the peaks are assigned to a single phase of α-Fe_2O_3.

use of a thin film compensates for the poor charge carrier transport ability of bulk α-Fe_2O_3 materials. Raman spectroscopy corroborated the phase assignment of the annealed film. Shifts were observed at 225, 293, 299, 407, 617, and 659 cm^{-1}. In agreement with the characterization based on PXRD measurements, this set of Raman modes matches well with those specific to α-Fe_2O_3[20] and were not observed in the Raman spectrum of the as-synthesized film (see Figure S7 in the Supporting Information). UV−vis absorption measurements of the annealed films also indicate the presence of hematite. Figure 5 shows the absorbance spectrum of a 19 nm iron oxide film grown by ALD using FeAMD on FTO. A small

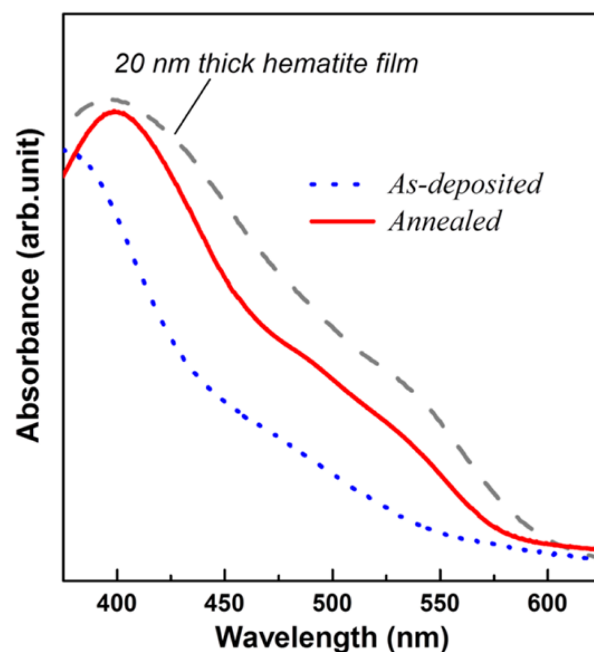

Figure 5. Optical absorption spectrum of 19 nm thick iron oxide thin film grown on FTO glass as-deposited (dashed blue) and after annealing at 500 °C in air (solid red). Gray-dashed line is a 20 nm thick hematite film grown using ferrocene-ozone ALD.

DOI: 10.1021/acsami.5b04043
ACS Appl. Mater. Interfaces 2015, 7, 16138−16142

shoulder characteristic of an α-Fe_2O_3 absorption is observed in the as-deposited film. When annealed, however, there is an increase in this absorption, and the shape becomes more characteristic of an α-Fe_2O_3 crystalline phase. Comparisons of films grown using the FeAMD precursor to α-Fe_2O_3 films grown using a standard ferrocene-ozone ALD route (Figure 5), reveal closely similar shapes for absorption spectra. Refer to Figure S8 for more detailed GIXRD of 19 nm films of α-Fe_2O_3 in the Supporting Information. Figure 6 shows photocurrent

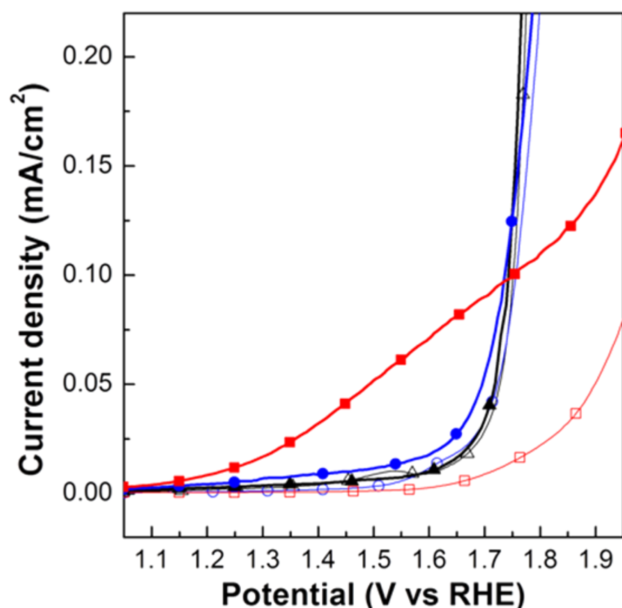

Figure 6. Current density−potential curves of α-Fe_2O_3 films with a thickness of 5 (black triangles), 14 (blue circles), and 19 (red squares) nm under illumination (filled markers) and in the dark (empty markers). These photocurrents were measured in 1 M NaOH aqueous solution with a platinum counter electrode and Ag/AgCl (saturated KCl) reference electrode, and the light source was a xenon lamp equipped with an AM 1.5 filter.

density−potential curves of the annealed films. For 19 nm thick film, the water oxidation photocurrent begins at about 1.2 V vs RHE and reaches 0.1 mA/cm^2 at 1.75 V vs RHE, and this confirms the photoelectrochemical activity for water oxidation reaction. However, 5 and 14 nm thick films exhibit almost no photocurrent response, which is hypothesized to be due to the low crystallinity of the very thin films.[30] From Figure 6, we can confirm the water oxidation activity of films grown using the FeAMD precursor resembles those grown using the ubiquitous ferrocene-ozone procedure,[13,14] but there is a lower hematite thickness limit for achieving photoelectrochemical activity. Further evaluation of the photoelectrochemical activity of thin films of hematite are ongoing.

In conclusion, we find that conformal and self-limiting films of FeO_x can be reliably grown using the FeAMD ALD precursor and water at moderately temperatures. Films prepared in this way can be converted to hematite by annealing in air, where evidence for conversion is provided by XRD, XPS, Raman, and electronic absorption spectroscopy measurements. FeAMD appears to be an excellent alternative to the formation of catalytically promising iron oxide materials due to its ease of use in commercial ALD systems, and its reliance upon thermally and chemically moderate conditions. While not explored here, the latter holds particular promise for integration of iron-oxide films and clusters with organic components in hybrid nanostructured materials.[22] We intend to report shortly on the synthesis and functional behavior of a few examples of such materials.

ASSOCIATED CONTENT

Supporting Information

Experimental details, in situ QCM study of reactor profile, supporting QCM, XPS, Raman spectrum, and XRD of this films. The Supporting Information is available free of charge on the ACS Publications website at DOI: 10.1021/acsami.5b04043.

AUTHOR INFORMATION

Corresponding Authors

*E-mail: o-farha@northwestern.edu.
*E-mail: j-hupp@northwestern.edu.

Author Contributions

All authors have given approval to the final version of the manuscript.

Notes

The authors declare no competing financial interest.

ACKNOWLEDGMENTS

This work was supported as part of the ANSER Center, an Energy Frontier Research Center funded by the U.S. Department of Energy, Office of Science, Office of Basic Energy Sciences, under Award DE-SC0001059. Ellipsometry, XPS, and Raman spectroscopy was performed in KECK II facilities of the NUANCE Center at Northwestern University. The NUANCE center is supported by NSF-NSEC, NSF-MRSEC, the KECK Foundation, the State of Illinois, and Northwestern University. This work made use of the J.B.Cohen X-ray Diffraction Facility supported by the MRSEC program of the National Science Foundation (DMR-1121262) at the Materials Research Center of Northwestern University. M.R. was supported by the Swiss National Science Foundation with an Early Postdoc Mobility Fellowship.

REFERENCES

(1) Bachmann, J.; Jing, J.; Knez, M.; Barth, S.; Shen, H.; Mathur, S.; Gösele, U.; Nielsch, K. Ordered Iron Oxide Nanotube Arrays of Controlled Geometry and Tunable Magnetism by Atomic Layer Deposition. *J. Am. Chem. Soc.* **2007**, *129*, 9554−9555.

(2) Katz, M. J.; Riha, S. C.; Jeong, N. C.; Martinson, A. B. F.; Farha, O. K.; Hupp, J. T. Toward Solar Fuels: Water Splitting with Sunlight and "Rust" ? *Coord. Chem. Rev.* **2012**, *256*, 2521−2529.

(3) Koo, B.; Xiong, H.; Slater, M. D.; Prakapenka, V. B.; Balasubramanian, M.; Podsiadlo, P.; Johnson, C. S.; Rajh, T.; Shevchenko, E. V. Hollow Iron Oxide Nanoparticles for Application in Lithium Ion Batteries. *Nano Lett.* **2012**, *12*, 2429−2435.

(4) Bjorksten, U.; Moser, J.; Gratzel, M. Photoelectrochemical Studies on Nanocrystalline Hematite Films. *Chem. Mater.* **1994**, *6*, 858−863.

(5) Hanson, K.; Losego, M. D.; Kalanyan, B.; Ashford, D. L.; Parsons, G. N.; Meyer, T. J. Stabilization of [Ru(bpy)2(4,4′-(PO3H2)bpy0]2+ on Mesoporous TiO2 with Atomic Layer Deposition of Al2O3. *Chem. Mater.* **2013**, *25*, 3−5.

(6) Lin, Y.; Xu, Y.; Mayer, M. T.; Simpson, Z. I.; McMahon, G.; Zhou, S.; Wang, D. Growth of p-type Hematite by Atomic Layer Deposition and its Utilization for Improved Solar Water Splitting. *J. Am. Chem. Soc.* **2012**, *134*, 5508−5511.

(7) Riha, S. C.; Klahr, B. M.; Tyo, E. C.; Seifert, S.; Vajda, S.; Pellin, M. J.; Hamann, T. W.; Brandon, A.; Martinson, F. Atomic Layer

Deposition of a Sub-Monolayer Catalyst for the Enhanced Photoelectrochemical Performance of Water Oxidation with Hematite Atomic Layer Deposition of a Sub-monolayer Catalyst for the Enhanced Photoelectrochemical Performance of Water Oxidation. *ACS Nano* **2013**, *7*, 2396−2405.
(8) Martinson, A. B. F.; DeVries, M. J.; Libera, J. a.; Christensen, S. T.; Hupp, J. T.; Pellin, M. J.; Elam, J. W. Atomic Layer Deposition of Fe_2O_3 using Ferrocene and Ozone. *J. Phys. Chem. C* **2011**, *115*, 4333−4339.
(9) Riha, S. C.; DeVries Vermeer, M. J.; Pellin, M. J.; Hupp, J. T.; Martinson, A. B. F. Hematite-Based Photo-Oxidation of Water using Transparent Distributed Current Collectors. *ACS Appl. Mater. Interfaces* **2013**, *5*, 360−367.
(10) Williams, V. O.; Demarco, E. J.; Katz, M. J.; Libera, J. a.; Riha, S. C.; Kim, D. W.; Avila, J. R.; Martinson, A. B. F.; Elam, W.; Pellin, M. J.; Farha, O. K.; Hupp, J. T. Fabrication of Transparent-Conducting-Oxide-Coated Inverse Opals as Mesostructured Architectures for Electrocatalysis Applications: A Case Study with NiO. *ACS Appl. Mater. Interfaces* **2014**, *6*, 12290−12294.
(11) George, S. M. Atomic Layer Deposition: An Overview. *Chem. Rev.* **2010**, *110*, 111−131.
(12) Miikkulainen, V.; Leskelä, M.; Ritala, M.; Puurunen, R. L. Crystallinity of Inorganic Films Grown by Atomic Layer Deposition: Overview and General Trends. *J. Appl. Phys.* **2013**, *113*, 021301.
(13) Kim, D. W.; Riha, S. C.; Demarco, E. J.; Martinson, A. B. F.; Farha, O. K.; Hupp, J. T. Greenlighting Photoelectrochemical Oxidation of Water by Iron Oxide. *ACS Nano* **2014**, *8*, 12199−12207.
(14) Klahr, B.; Gimenez, S.; Fabregat-Santiago, F.; Bisquert, J.; Hamann, T. W. Electrochemical and Photoelectrochemical Investigation of Water Oxidation with Hematite Electrodes. *Energy Environ. Sci.* **2012**, *5*, 7626.
(15) Klahr, B.; Hamann, T. Water Oxidation on Hematite Photoelectrodes: Insight into the Nature of Surface States through In Situ Spectroelectrochemistry. *J. Phys. Chem. C* **2014**, *118*, 10393−10399.
(16) Lie, M.; Fjellvåg, H.; Kjekshus, a. Growth of Fe2O3 Thin Films by Atomic Layer Deposition. *Thin Solid Films* **2005**, *488*, 74−81.
(17) Martinson, A. B. F.; DeVries, M. J.; Libera, J. a.; Christensen, S. T.; Hupp, J. T.; Pellin, M. J.; Elam, J. W. Atomic Layer Deposition of Fe2O3 using Ferrocene and Ozone. *J. Phys. Chem. C* **2011**, *115*, 4333−4339.
(18) Rooth, M.; Johansson, A.; Kukli, K.; Aarik, J.; Boman, M.; Hårsta, A. Atomic layer Deposition of Iron Oxide Thin Films and Nanotubes using Ferrocene and Oxygen as Precursors. *Chem. Vap. Deposition* **2008**, *14*, 67−70.
(19) Scheffe, J. R.; Francés, A.; King, D. M.; Liang, X.; Branch, B. a.; Cavanagh, A. S.; George, S. M.; Weimer, A. W. Atomic Layer Deposition of Iron(III) Oxide on Zirconia Nanoparticles in a Fluidized Bed Reactor using Ferrocene and Oxygen. *Thin Solid Films* **2009**, *517*, 1874−1879.
(20) Riha, S. C.; Racowski, J. M.; Lanci, M. P.; Klug, J. A.; Hock, A. S.; Martinson, A. B. F. Phase Discrimination Through Oxidant Selection in Low-Temperature Atomic Layer Deposition of Crystalline Iron Oxides. *Langmuir* **2013**, *29*, 3439−3445.
(21) Avila, J. R.; DeMarco, E. J.; Emery, J. D.; Farha, O. K.; Pellin, M. J.; Hupp, J. T.; Martinson, A. B. F. Real-Time Observation of Atomic Layer Deposition Inhibition: Metal Oxide Growth on Self-Assembled Alkanethiols. *ACS Appl. Mater. Interfaces* **2014**, *6*, 11891−11898.
(22) Mondloch, J. E.; Bury, W.; Fairen-Jimenez, D.; Kwon, S.; Demarco, E. J.; Weston, M. H.; Sarjeant, A. a.; Nguyen, S. T.; Stair, P. C.; Snurr, R. Q.; Farha, O. K.; Hupp, J. T. Vapor-Phase Metalation by Atomic Layer Deposition in a Metal-Organic Framework. *J. Am. Chem. Soc.* **2013**, *135*, 10294−10297.
(23) Klug, J. A.; Becker, N. G.; Riha, S. C.; Martinson, A. B. F.; Elam, J. W.; Pellin, M. J.; Proslier, T. Low Temperature Atomic Layer Deposition of Highly Photoactive Hematite using Iron(iii) Chloride and Water. *J. Mater. Chem. A* **2013**, *1*, 11607−11613.
(24) Lim, B. S.; Rahtu, A.; Gordon, R. G. Atomic Layer Deposition of Transition Metals. *Nat. Mater.* **2003**, *2*, 749−54.
(25) Riha, S. C.; Jin, S.; Baryshev, S. V.; Thimsen, E.; Wiederrecht, G. P.; Martinson, A. B. F. Stabilizing Cu2S for Photovoltaics One Atomic Layer at a Time. *ACS Appl. Mater. Interfaces* **2013**, *5*, 10302−10309.
(26) Riha, S. C.; Libera, J. a.; Elam, J. W.; Martinson, A. B. F. Design and Implementation of an Integral Wall-Mounted Quartz Crystal Microbalance for Atomic Layer Deposition. *Rev. Sci. Instrum.* **2012**, *83*, 094101.
(27) Aarik, J.; Aidla, A.; Mändar, H.; Sammelselg, V. Anomalous Effect of Temperature on Atomic Layer Deposition of Titanium Dioxide. *J. Cryst. Growth* **2000**, *220*, 531−537.
(28) Heo, J.; Hock, A. S.; Gordon, R. G. Low Temperature Atomic Layer Deposition of Tin Oxide. *Chem. Mater.* **2010**, *22*, 4964−4973.
(29) Examination of the growth mechanism and structure of FeO_x grown with oxygen is beyond the scope of this study, but this method presents an interesting opportunity to grow iron oxide films at higher oxidation states.
(30) Klahr, B. M.; Martinson, A. B. F.; Hamann, T. W. Photoelectrochemical Investigation of Ultrathin Film Iron Oxide Solar Cells Prepared by Atomic Layer Deposition. *Langmuir* **2011**, *27*, 461−468.

DOI: 10.1021/acsami.5b04043
ACS Appl. Mater. Interfaces 2015, 7, 16138−16142